Cyber Network Design for Secondary Frequency Regulation: A Spectral Approach

Linqi Guo, Changhong Zhao, and Steven H. Low

***Abstract*—We present a preliminary theoretical framework based on spectral graph theory that captures how the cyber topology of a distributed secondary frequency control scheme impacts the stability, optimality, and transient performance of our power system as a cyber-physical network. We show that a collection of polynomials defined in terms of the cyber and physical Laplacian eigenvalues encode information on the interplay between cyber and physical networks. It is demonstrated that to understand the impact of adding cyber connectivity, one should separate the low-damping and high-damping regimes. Although adding cyber connectivity always improves the performance for high-damping systems, it is not the case for low-damping scenarios. Based on the theoretical study, we discuss how a good cyber network should be designed. Our empirical study shows that for practical systems, the number of communication channels that is needed to achieve near-optimal performance is usually less than twice the number of buses.**

I. Introduction

Frequency regulation maintains the frequency of a power system around its nominal value when demand or supply fluctuates. It is traditionally implemented by generators through three mechanisms [1], [2]: a) primary frequency regulation, also known as droop control, that aims to stabilize the system after a disturbance but does not necessarily brings the frequency back to the nominal value; b) secondary frequency regulation, also known as Automatic Generation Control (AGC), that sets the generator operating point in a centralized manner based on available generator reserves and drives the system back to the nominal frequency; c) tertiary frequency regulation, also known as economic dispatch, that optimizes the economic efficiency subject to security constraints.

Because of the increasing penetration of distributed energy resources that introduces random disturbances in power supply and demand, a new paradigm with emphasis on load-side participation has been recently studied in a series of experimental evaluation [3], [4] and theoretical work [5]–[15]. It has been shown that compared to AGC, the power grid equipped with load-side participation typically responds faster and the disturbances are more localized [8]–[11]. See [16] for extensive references to recent literature on frequency control.

Linqi Guo and Steven H. Low are with the Department of Computing and Mathematical Sciences, California Institute of Technology, Pasadena, CA, 91125. Email: {lguo, slow}@caltech.edu. Changhong Zhao is with the National Renewable Energy Laboratory, Golden, CO, 80401. Email: Changhong.Zhao@nrel.gov.

The authors thank Professor Janusz Bialek from Skoltech for helpful discussions. This work has been supported by Resnick Fellowship, Linde Institute Research Award, DOE through the ENERGISE program (Award #DE-EE-0007998), NSF grants through CCF 1637598, ECCS 1619352, CNS 1545096, ARPA-E grant through award DE-AR0000699 (NODES) and GRID DATA, DTRA through grant HDTRA 1-15-1-0003 and Skoltech through collaboration agreement 1075-MRA.

As with the conventional centralized AGC, the controllers proposed for secondary frequency regulation in recent studies [10]–[12], [15], [17] usually require the information on power supply and demand mismatch to be communicated across the physical network. Communications of this type require dedicated channels that can be different from the physical connections and the network formed by such channels is referred to as the cyber network. In contrast to the physical network that transports power, a cyber network transports information and determines the states available for control at each bus. Most existing studies [10], [12], [17] design the cyber network to have the same topology as the physical network, despite their different purposes and implementations. Such association, although natural, can be less practical in structure preserving models where not all the buses can communicate with each other or are controllable [18]. This poses constraints on how cyber topologies can be designed. We are hence interested in understanding how different cyber network designs impact the stability, optimality, and transient performance of the power system.

The separation of cyber topology from the physical topology is not only a constraint, but can also be an extra degree of freedom in the load-side controller design. We present a preliminary theoretical framework based on spectral graph theory for the analysis of our power system as a cyber-physical network. Our contributions can be summarized as follows: a) We demonstrate that the interaction between cyber and physical networks can be captured by the corresponding Laplacian eigenvalues through a collection of polynomials which we coin as the spectral crossing polynomials; b) We show that to understand the impact of adding cyber connectivity to a power system, we should separate the low-damping and high-damping regimes. Although adding cyber connectivity always improves the performance for high-damping systems, it is not the case for low-damping systems (such as one with extensive renewable penetration); c) Based on the theoretical study, we discuss and evaluate how to design cyber networks. Through empirical study, we show that for practical systems, the number of communication channels that we need to achieve near-optimal performance is usually less than twice the number of buses.

Despite the fact that our analysis poses strong assumptions on the system parameters and some critical values for applications (such as the boundary between low-daming and high-damping regimes) may not be directly computable from the theory, this framework reveals useful and nontrivial insights that can help system design and we hope our results can motivate more research along this thread. Due to space limitation, we focus on secondary frequency controller in the sequel and interested readers are referred to our online

report [19] for more dicussions on the impact of network topologies on primary frequency control. The rest of this paper is organized as follows. In Section II, we present our network model and review relevant concepts from spectral graph theory. In Section III, we present our characterization on the cyber and physical networks interaction and how they impact the system performance through the corresponding Laplacian eigenvalues. In Section IV, we discuss how a good cyber network should be designed. In Section V, we demonstrate our theoretical results on a large-scale ring network and on IEEE 39-bus New England interconnection testbed. We conclude in Section VI.

II. Model and Problem Setup

In this section, we present the network model as adopted in [9], [10] and the controller from [10], which will be refined in our study to incorporate cyber network design. We also review relevant concepts from spectral graph theory.

Let $\mathbb{R}$ and $\mathbb{C}$ denote the set of real and complex numbers, respectively. For a set $\mathcal{N}$, its cardinality is denoted as $|\mathcal{N}|$. For two matrices A, B with proper dimensions, $[A\ B]$ means the concatenation of A, B in a row, and $[A; B]$ means the concatenation of A, B in a column. A variable without subscript usually denotes a vector with appropriate components, e.g., $\omega = (\omega_j, j \in \mathcal{N}) \in \mathbb{R}^{|\mathcal{N}|}$. For any matrix A, we denote A^T as its transpose and denote $\mathrm{kernel}(A)$ as its kernel. For a time-dependent signal $\omega(t)$, we use $\dot{\omega}$ to denote its time derivative $\frac{d\omega}{dt}$. The identity matrix of dimension $n \times n$ is denoted as I_n.

We use $\mathcal{G}^p = (\mathcal{N}, \mathcal{E}^p)$ and $\mathcal{G}^c = (\mathcal{N}, \mathcal{E}^c)$ to describe the physical transmission network and cyber network respectively, where $\mathcal{N} = \{1, \ldots, n\}$ is the set of buses, $\mathcal{E}^p \subset \mathcal{N} \times \mathcal{N}$ is the set of physical transmission lines and $\mathcal{E}^c \subset \mathcal{N} \times \mathcal{N}$ is the set of communication channels. Note that we do not require the cyber graph $\mathcal{G}^c$ to be a subgraph of $\mathcal{G}^p$. In other words the cyber network may contain communication channels connecting non-neighboring buses in the physical network and physical neighbors may not be able to communicate. Recent studies [10], [12], [17] assume $\mathcal{E}^c = \mathcal{E}^p$, which is a special case of the model considered here. The terms bus/node and line/edge/channel are used interchangeably in this paper. We assume without loss of generality that both $\mathcal{G}^p$ and $\mathcal{G}^c$ are connected and simple (without self-loops). An edge is denoted either as e or (i, j) and we further assign arbitrary orientations to both the physical links $\mathcal{E}^p$ and cyber links $\mathcal{E}^c$.

Let n, m^p be the number of buses and physical transmission lines respectively. The incidence matrix of $\mathcal{G}^p$ is the $n \times m^p$ matrix C^p defined as

$$C^p_{ie} = \begin{cases} 1 & \text{if node } i \text{ is the source of } e, e \in \mathcal{E}^p \\ -1 & \text{if node } i \text{ is the target of } e, e \in \mathcal{E}^p \\ 0 & \text{otherwise} \end{cases}$$

The incidence matrix C^c for the cyber graph $\mathcal{G}^c$ is defined similarly. For each bus $j \in \mathcal{N}$, we denote its frequency deviation as ω_j and denote the inertia constant as $M^p_j > 0$. The symbol P^m_j is overloaded to denote the mechanical power injection if j is a generator bus and denote the aggregate power injection from uncontrollable load if j is a load bus. For a generator bus, we model the droop control as $D_j\omega_j$ with $D_j \geq 0$ and for load buses, we use the same symbol to denote an aggregated frequency sensitive load. For each transmission line $(i, j) \in \mathcal{E}$, denote by P_{ij} the branch flow deviation and denote by B^p_{ij} the line susceptance. With these notations, the swing and power flow dynamics is given by

$$M^p_j \dot{\omega}_j = P^m_j - D_j\omega_j - d_j - \sum_{e \in \mathcal{E}} C^p_{je} P_e, \quad j \in \mathcal{N} \quad \text{(1a)}$$

$$\dot{P}_{ij} = B^p_{ij}(\omega_i - \omega_j), \qquad (i, j) \in \mathcal{E}^p \quad \text{(1b)}$$

We refer the readers to [9], [10] for more detailed justification and derivation of this model.

The key idea in [10] is to capture supply-demand mismatch at each bus using virtual variables λ_j and distribute such information through cyber channels to physical neighbors so that the aggregate mismatch information mixes throughout the grid. The mixing dynamics via cyber channels is captured by virtual flow variables R_{ij}. The controller is designed in a way such that the physical dynamics (1a) and (1b) equipped with the feedback control forms a primal-dual algorithm to solve a certain Optimal Load Control problem. Putting M^c_j, K_j and B^c_{ij} to be positive gain constants, the controller dynamics from [10] is given as

$$M^c_j \dot{\lambda}_j = P^m_j - d_j - \sum_{e \in \mathcal{E}^c} C^c_{je} R_e, \qquad j \in \mathcal{N} \quad \text{(1c)}$$

$$\dot{R}_{ij} = B^c_{ij}(\lambda_i - \lambda_j), \qquad (i, j) \in \mathcal{E}^c \quad \text{(1d)}$$

$$d_j = K_j(\omega_j + \lambda_j), \qquad j \in \mathcal{N} \quad \text{(1e)}$$

In [10], the cyber network and physical network coincide, that is $\mathcal{E}^c = \mathcal{E}^p$. We relax this assumption in our study so we can understand the impact of cyber topology on the performance of the system dynamics (1).

Now using x to denote the system state $x = [\omega; \lambda; P; R]$, and putting M^p, M^c, D, B^p, B^c and K to be the diagonal matrices with M^p_j, M^c_j, $D_j + K_j$, B^p_{ij}, B^c_{ij} and K_j as diagonal entries respectively, we can rewrite the system dynamics in state-space form

$$\dot{x} = Ax + \begin{bmatrix} (M^p)^{-1} \\ (M^c)^{-1} \\ 0 \\ 0 \end{bmatrix} P^m \quad (2)$$

where A is given as

$$\begin{bmatrix} -(M^p)^{-1}D & -(M^p)^{-1}K & -(M^p)^{-1}C^p & 0 \\ -(M^c)^{-1}K & -(M^c)^{-1}K & 0 & -(M^c)^{-1}C^c \\ B^p(C^p)^T & 0 & 0 & 0 \\ 0 & B^c(C^c)^T & 0 & 0 \end{bmatrix}$$

and is referred to as the system matrix in the sequel. We emphasize that the variables $[\omega; \lambda; P; R]$ denote deviations from their nominal values so $x(t) = 0$ means the system is in its nominal state at time t, though it is not an equilibrium point unless $P^m = 0$.

For any node $i \in \mathcal{N}$, we denote the set of its physical neighbors as $N^p(i)$. The (susceptance weighted) graph Laplacian matrix of $\mathcal{G}^p$ is the $n \times n$ symmetric (and thus diagonalizable) matrix $L^p = C^p B^p (C^p)^T$, which is explicitly given by

$$L^p_{ij} = \begin{cases} -B^p_{ij} & i \neq j, (i, j) \in \mathcal{E}^p \text{ or } (j, i) \in \mathcal{E}^p \\ \sum_{k \in N^p(i)} B^p_{ik} & i = j \\ 0 & \text{otherwise} \end{cases}$$

If the graph $\mathcal{G}^p$ is connected, then L^p has rank $n-1$, and any principal minor of L^p is invertible [20]. For any vector $x \in \mathbb{R}^n$, we have

$$x^T L^p x = \sum_{(i,j)\in\mathcal{E}} B^p_{ij}(x_i - x_j)^2 \geq 0$$

This implies that L^p is positive semidefinite. We denote its eigenvalues as $0 = \lambda^p_1 < \lambda^p_2 \leq \cdots \leq \lambda^p_n$. The Laplacian matrix L^c of the cyber graph $\mathcal{G}^c$ and its eigenvalues $0 = \lambda^c_1 < \lambda^c_2 \leq \cdots \leq \lambda^c_n$ are defined similarly.

Our analysis builds upon two assumptions:

1) **Homogeneity.** We require the buses to be homogeneous in the sense that $M^p = \mu^p I_n$, $M^c = \mu^c I_n$, $D = (\delta+\kappa)I_n$ and $K = \kappa I_n$ for some $\mu^p, \mu^c, \delta, \kappa > 0$[1]. Our results can be readily generalized to the case where the system paramters are heterogeneous but proportional to system ratings following an approach similar to [21], in which case the notations in our results would be more complicated. We believe such complication does not reveal new insights and thus opt not to doing so here.
2) **Commutativity.** We require the Laplacian matrices L^p and L^c to be commutative: $L^pL^c = L^cL^p$. Although the practical meaning of this assumption is less clear, studies in [22], [23] show that the commutativity property holds at least approximately in some settings.

These two assumptions allow us to decompose the system (2) through spectral crossing polynomials (which we define in Section III) and present the main conclusions in a more transparent and interpretable fashion.

III. Main Results

In this section, we characterize how the cyber topology $\mathcal{G}^c$ impacts the stability of (2) and its convergence rate if (2) is stable.

A. Characterization of System Modes

We first provide a characterization of the system modes. That is, we compute the eigenvalues of the system matrix A, which determine whether the system is stable, and if so, how fast it converges to an equilibrium state. We introduce the concept of spectral crossing polynomials, which encode information on how the cyber and physical topologies, as captured by the corresponding Laplacian eigenvalues, interact with each other and impact the overall system performance. Recall n is the number of buses.

Definition III.1 (Spectral Crossing Polynomial)**.** Let $0 = \lambda^p_1 < \lambda^p_2 \leq \ldots \leq \lambda^p_n$ and $0 = \lambda^c_1 < \lambda^c_2 \leq \ldots \leq \lambda^c_n$ be the Laplacian eigenvalues of $\mathcal{G}^p$ and $\mathcal{G}^c$ respectively. For $1 \leq i \leq n$, the i-th spectral crossing polynomial of (2) is defined to be the quartic polynomial

$$\chi_i(t) := \left(\mu^p t^2 + (\delta+\kappa)t + \lambda^p_i\right)\left(\mu^c t^2 + \kappa t + \lambda^c_i\right) - \kappa^2 t^2$$

Theorem III.2. *Let $0 = \lambda^p_1 < \lambda^p_2 \leq \ldots \leq \lambda^p_n$ and $0 = \lambda^c_1 < \lambda^c_2 \leq \ldots \leq \lambda^c_n$ be the Laplacian eigenvalues of $\mathcal{G}^p$ and $\mathcal{G}^c$ respectively and assuming $L^pL^c = L^cL^p$. Then:*

1) *0 is an eigenvalue of A of multiplicity $m^p + m^c - 2n + 2$*
2) *The first spectral crossing polynomial $\chi_1(t)$ has two nonzero roots, both of which are real, strictly negative, and they are eigenvalues of A*
3) *For $2 \leq i \leq n$, all the four roots of the i-th spectral crossing polynomial $\chi_i(t)$ are eigenvalues of A*

When $m^p + m^c - 2n + 2 = 0$, or equivalently when both $\mathcal{G}^p$ and $\mathcal{G}^c$ are trees, item 1) in Theorem III.2 is understood to mean that the system matrix A does not have 0 as an eigenvalue. Laplacian eigenvalues of a graph measure its connectivity from an algebraic perspective, and larger Laplacian eigenvalues suggest stronger connectivity. See our online report [19] for more discussions. Theorem III.2 thus implies the cyber topology impacts the convergence properties of (2) precisely through the Laplacian eigenvalues.

B. Convergence and Equilibrium

We now show that the system (2) converges as long as the cyber network $\mathcal{G}^c$ is connected, which allows us to optimize the cyber topology without losing the asymptotic stability of (2). Although in principle one can explicitly solve all the roots of $\chi_i(t)$ as a quartic polynomial, the general formulae are complicated and hard to track analytically. Instead, we will prove relevant properties of these roots as functions of the cyber Laplacian eigenvalues λ^c_i and these properties are sufficient for our understanding of system convergence and cyber network design.

Lemma III.3. *Assuming $L^pL^c = L^cL^p$, all nonzero eigenvalues of A have negative real parts.*

This result implies that under the commutativity assumption, the system (2) is marginally stable. That is, assuming the system initial state $x(0)$ is not in the kernel of A (or if $x(0) = 0$), under zero input $P^m = 0$ we have that (2) converges to the nominal state $\lim_{t\to\infty} x(t) = 0$. The technical condition on the commutativity of L^p and L^c is sufficient but very likely unnecessary (based on physical intuition) and we are still investigating how it can be relaxed. If both $\mathcal{G}^p$ and $\mathcal{G}^c$ are trees, then Theorem III.2 implies that A does not have zero eigenvalue and thus (2) is asymptotically stable. When at least one of $\mathcal{G}^p$ or $\mathcal{G}^c$ is a mesh network, we can explicitly compute the kernel of A as follows.

Lemma III.4. *The kernel of A is given as*

$$\{[0;0;P;R] : P \in \text{kernel}(C^p), R \in \text{kernel}(C^c)\}$$

The kernel of C^p corresponds to circulating branch flows P that are balanced everywhere, that is $\sum_{j\in N^p(i)} P_{ij} = 0$ for all $i \in \mathcal{N}$ and thus there is neither a source (for which $\sum_{j\in N^p(i)} P_{ij} > 0$) nor a sink (for which $\sum_{j\in N^p(i)} P_{ij} < 0$). The kernel of C^c can be interpreted similarly. Thus the only states that can persist in system (2) are circulating balanced branch flows and virtual flows. As long as $P(0) = R(0) = 0$ (i.e. physical and virtual branch flows are at their nominal values before the disturbance at $t = 0_+$), the system (2) is guaranteed to converge to the equilibrium state $\lim_{t\to\infty} x(t) = 0$ (under zero input $P^m = 0$). That is, as long as no circulating flows exist at the initial state, there will be no circulating flows at the steady state.

[1]Note that for notation simplicity we absorbed both the damping δ and controller gain κ into the matrix D. We do not require κ to always be smaller than the damping level δ in our results.

From Lemma III.3 and III.4 we know that the system (2) restores to the nominal state after impulse disturbances (which affects the initial state $x(0)$). They also imply the system (2) converges to an equilibrium point, which can be different from the nominal state, under a step disturbance. The following result shows that with the controller (1c)-(1e), secondary frequency regulation is always attained at the equilibrium.

Lemma III.5. *Under a step input $P^m(t) = P^m$, any equilibrium point $x^* = [\omega^*; \lambda^*; P^*; R^*]$ of (2) satisfies $\omega^* = 0$.*

Our characterizations on the stability of (2) can then be summarized as follows.

Theorem III.6. *Assume the initial state of (2) satisfies $P(0) = R(0) = 0$. Then under a step input $P^m(t) = P^m$, we have:*

1) *For any connected cyber network $\mathcal{G}^c$, the system (2) asymptotically converges to an equilibrium state*
2) *When the system (2) converges to the equilibrium state $x^* = [\omega^*, \lambda^*, P^*, R^*]$, secondary frequency regulation is attained:*

$$\omega_i^* = 0, \quad \forall i \in \mathcal{N}$$

C. Impact of System Damping

Next we discuss a bifurcation phenomenon on the impact of cyber topology to the convergence rate of system (2) under different system damping level δ.

Definition III.7 (Principal Rate)**.** Consider a spectral crossing polynomial $\chi_i(t)$ with $i \geq 2$. Let $\mathrm{Re}(\chi_i^{-1}(0))$ be the set of real parts of its roots (all of them are nonzero). The principal rate of $\chi_i(t)$, denoted as ρ_i, is defined to be

$$\rho_i := \max\left(\mathrm{Re}(\chi_i^{-1}(0))\right) < 0$$

For $i = 1$, the principal rate of χ_1 is defined to be its least negative root [2]

$$\rho_1 := \max\left(y \in \chi_1^{-1}(0) : y \neq 0\right) < 0$$

For a spectral crossing polynomial χ_i, its principal rate encodes the slowest convergent mode of system (2) coming from χ_i. Therefore to obtain faster convergence, we should design the system so that ρ_i's are as negative as possible. For χ_i, by designing the cyber network $\mathcal{G}^c$, we effectively choose different Laplacian eigenvalues λ_i^c, and hence it is of interest to see how $\rho_i(\lambda_i^c)$ behaves as a function of λ_i^c. Since for any connected $\mathcal{G}^c$, the smallest cyber Laplacian eigenvalue $\lambda_1^c = 0$, we know ρ_1 is independent of λ_i^c so we will focus on the case $i \geq 2$ in the following.

Theorem III.8. *Fix the physical Laplacian eigenvalues λ_i^p and put $\hat{\lambda}_i^p := \frac{\mu^c \lambda_i^p}{\mu^p}$. For each $i \geq 2$, there is a critical damping level $\overline{\delta}_i$ such that:*

1) *For $\delta \in [0, \overline{\delta}_i)$, there exists $\overline{\lambda}_i^p$ satisfying $0 < \overline{\lambda}_i^p < \hat{\lambda}_i^p$ so that $\rho_i(\lambda_i^c)$ is decreasing on $\left[0, \overline{\lambda}_i^p\right]$ and $[\hat{\lambda}_i^p, \infty)$ and increasing on $\left(\overline{\lambda}_i^p, \hat{\lambda}_i^p\right)$. Moreover,*

$$\rho_i\left(\hat{\lambda}_i^p\right) > \lim_{\lambda_i^c \to \infty} \rho_i(\lambda_i^c)$$

[2]One can show that all roots of χ_1 are real.

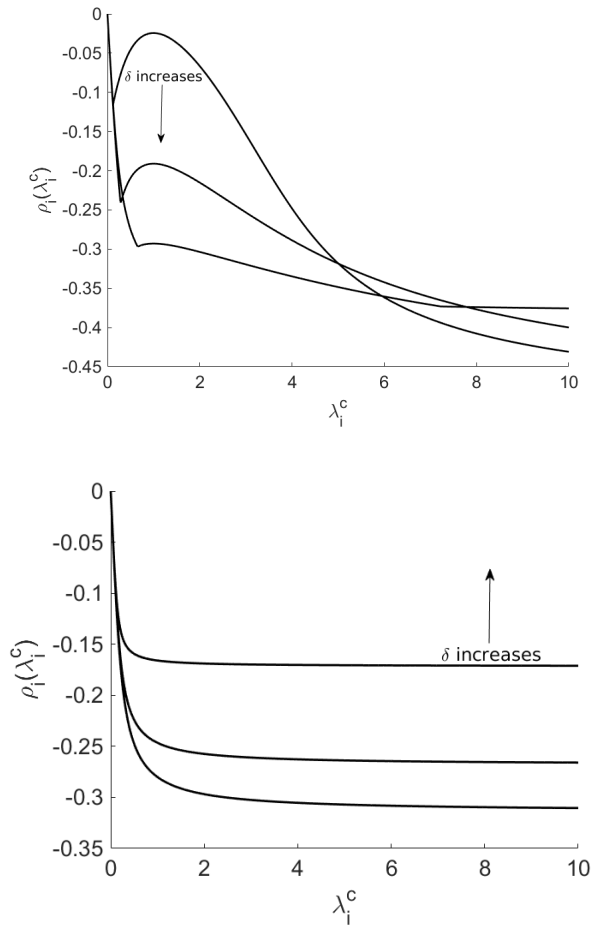

Figure 1. Demonstration of the principal rate $\rho_i(\lambda_i^c)$ for different damping levels with $\mu^c = \mu^p = \lambda_i^p = 1$. (a) For $\delta \in \left[0, \overline{\delta}_i\right)$, the curve $\rho_i(\lambda_i^c)$ has two extreme points. The curve stationary point at $\overline{\lambda}_i^p$ moves downward as δ increases. (b) For $\delta \in \left[\overline{\delta}_i, \infty\right)$, the function $\rho_i(\lambda_i^c)$ is monotonically decreasing. The curve moves upward as δ increases.

2) *For $\delta \in \left[\overline{\delta}_i, \infty\right)$, $\rho_i(\lambda_i^c)$ is strictly decreasing in λ_i^c*

This result tells us that to understand the impact of cyber topologies on the convergence rate of (2), we should separate the low-damping and high-damping regimes. Recall that increasing the cyber Laplacian eigenvalues λ_i^c corresponds to adding connectivity to the cyber graph $\mathcal{G}^c$. We then see that when the system damping is not strong enough, adding cyber connectivity does not always improve the convergence rate. In fact, when $\mu^p = \mu^c$, choosing the cyber network $\mathcal{G}^c$ to be the same as the physical network $\mathcal{G}^p$ is locally the worst design in the sense that by choosing any other topology "nearby"[3], we can obtain faster convergence of the system (2). In contrast, for a system where damping is strong enough, adding cyber connectivity always increases the convergence rate. In either case, to obtain a good performance of the system (2) in terms of convergence rate, we should always choose cyber topologies

[3]We measure the distance between two topologies by the sup norm of the difference in their ordered eigenvalues. It can be shown that this distance defines a metric space over all topologies quotient the isospectral equivalence relation.

with sufficiently large λ_i^c. See Figure 1 for a demonstration of this bifurcation behavior.

IV. Design of Cyber Network

In this section, we present two tradeoffs in cyber network design for system (2) and discuss an algorithm for cyber topology design. Recall we have shown in Theorem III.8 that regardless of the system damping level, starting from a cyber network such that $\lambda_i^c = \hat{\lambda}_i^p$ for all i, which is the case when the cyber and physical topologies coincide and $\mu^p = \mu^c$, one can always improve the convergence rate of the system (2) by increasing the cyber Laplacian eigenvalues. There are two degrees of freedom one can explore to achieve this: 1) the virtual reactances B^c, 2) the cyber topology $\mathcal{G}^c$.

A. Tradeoff between Convergence Rate and Noise Suppression

It is tempting to take a similar approach to the Markov chain mixing rate optimization in [24] and solve the following optimization problem

$$\begin{array}{ll} \max & \operatorname{tr}\left(C^c B^c (C^c)^T\right) \\ \text{s.t.} & B_{ij}^c \geq 0, \quad \forall i,j \in \mathcal{N} \end{array}$$

to search for the optimal virtual reactances. However, one quickly see that this optimization is ill-defined in the sense that the optimal solution is given as $B_{ij}^c = \infty$, or in other words, we should pick the virtual reactances B_{ij}^c as large as possible. Such large gains amplify measurement noise through the network and are harmful to system robustness. Therefore in terms of the virtual reactance selection, there is a tradeoff between fast convergence and noise suppression.

B. Tradeoff between Convergence Rate and Communication Overhead

It can be shown that the Laplacian eigenvalues are monotonic with respect to the graph topologies. That is, suppose $\mathcal{G}_1$ is a subgraph of $\mathcal{G}_2$ with the same set of vertices, and denote the Laplacian eigenvalues of $\mathcal{G}_1$ and $\mathcal{G}_2$ as $0 = \lambda_{11} < \lambda_{12} \leq \ldots \leq \lambda_{1n}$ and $0 = \lambda_{21} < \lambda_{22} \leq \ldots \leq \lambda_{2n}$ respectively, then $\lambda_{1i} \leq \lambda_{2i}$ for any i, and there exists at least one i^* such that $\lambda_{1i^*} < \lambda_{2i^*}$. See [25] for more details. Therefore to obtain the largest eigenvalues, we should always pick the "largest" graph, which is the complete graph K_n, as the cyber topology. However, having a complete graph means more communication channels are required for the controllers to exchange state information, which incurs more communication overhead compared to existing controllers [10], [11], [17]. As a result, in terms of topology design, there is a tradeoff between fast convergence and communication overhead.

C. Small-world Network

Fortunately, for many practical systems, it is possible to increase the cyber Laplacian eigenvalues without increasing the communication overhead as in [10] by exploiting the so-called ultra-fast consensus network [26]. The ultra-fast consensus network generalizes the classical Watts-Strogatz small-world network model [27] to arbitrary graphs, and is experimentally demonstrated in [26] to be able to significantly increase the Laplacian eigenvalues for many graphs. The key idea in [26], [27] is to exploit random rewiring of the links so that the resulting graph has enough "randomness" and thus large connectivity. We present our evaluation results of using the ultra-fast consensus network for cyber topology design in Section V and the readers are referred to [26] for more detailed discussions on the algorithm itself.

V. Evaluation

In this section, we evaluate our theoretical results from Section III on practical systems.

A. Faster Mixing over Ring Network

To demonstrate the improved convergence rate when the cyber network is carefully designed, we simulate the dynamics (2) on a ring network of 300 buses, as shown in Figure 5(a). We first add a 1 pu load to one of the buses and look at the frequency trajectories when the cyber network has the same ring topology (i.e., with 300 links in the communication graph). The result is shown in Figure 5(b). Then we use the algorithm in [26] to generate a small-world cyber network, whose topology is shown in Figure 5(c), with the same number (i.e., 300) of communication channels but larger Laplacian eigenvalues and observe the resulting frequency trajectories under the same disturbance. The result is shown in Figure 5(d). In this special case, the system (2) drives itself back to the nominal state about five times faster when the cyber network is carefully designed. We expect such benefits to be more significant when the network is of larger scale.

B. Low Damping Regime

We showed in Theorem III.8 that for a network with relatively low damping level (which will be the case for future grids with extensive renewable penetration), compared to the configuration where the cyber topology coincides with the physical topology, we can in fact achieve better convergence rate of (2) if we use fewer communication channels. To verify this counter-intuitive behavior, we simulate the dynamics (2) on the IEEE 39-bus New England interconnection testbed (See Figure 2), whose system parameters are taken from the MATPOWER package [28] but with only one-tenth of the real damping constants D_j. Moreover, unlike our theoretical study where the buses are homogeneous, the system parameters in this evaluation are heterogeneous. To carry out the simulation, we first add an additional load of 1 pu to bus 30 and observe the frequency trajectories of the system, which are shown in Figure 3(a). Then we remove the communication channels $(3, 18), (18, 17), (4, 14)$ as indicated by crosses in Figure 2 and look at the system trajectories under the same disturbance. One can observe that in this specific example with low damping level, we can in fact make (2) more stable and more responsive by using weaker cyber connectivity.

C. How many links are enough?

In this experiment, we evaluate how the number of communication channels can affect the overall convergence rate of (2) in an ultra-fast consensus network. To do so, we run the algorithm in [26] over the IEEE 39-bus testbed to generate small-world cyber networks with different number of communication channels and compute the dominant real part of the system matrix A (the least negative nonzero real part among all eigenvalues of A) in each case. To account for the randomness in the algorithm from [26], we repeat the experiment 100

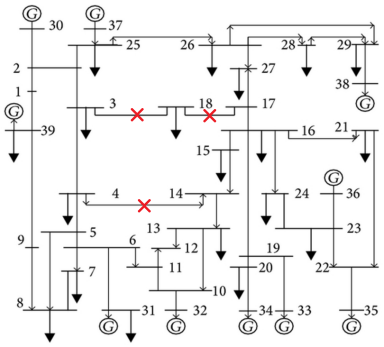

Figure 2. Line diagram of the IEEE 39-bus New England interconnection testbed. The crossed lines are removed in the second part experiment of Section V-B.

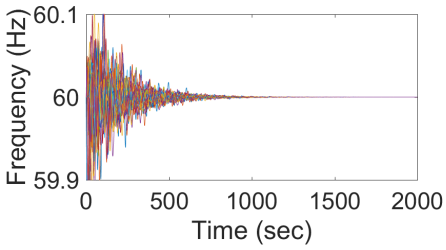

(a) Cyber and physical topologies coincide.

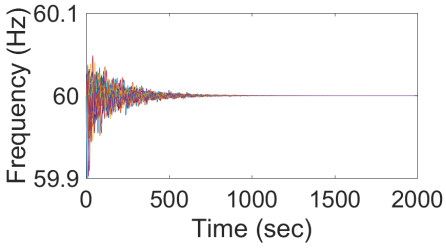

(b) The cyber topology with links $(3, 18), (18, 17), (4, 14)$ removed.

Figure 3. Frequency trajectories of the IEEE 39-bus New England interconnection testbed for two different cyber topologies.

times for each number of communication channels and collect the average and max/min statistics. The simulation results are shown in Figure 4, in which we have also included the case where we choose the physical topology (consisting of 46 links) for the cyber network and a lower bound[4] computed from having $\lambda_i^c \to \infty, i = 2, 3, \ldots, n$, for comparison. As one can see from the figure, with about 60 communication channels or roughly 1.5 times the number of buses in this testcase, the

[4]Although we have only proved the optimal convergence rate of (2) is achieved at infinite large cyber Laplacian eigenvalues *provided the homogeneity and commutativity assumptions in Section II hold*, it is possible to show that this statement regarding optimality is still true even if neither of the assumptions is posed.

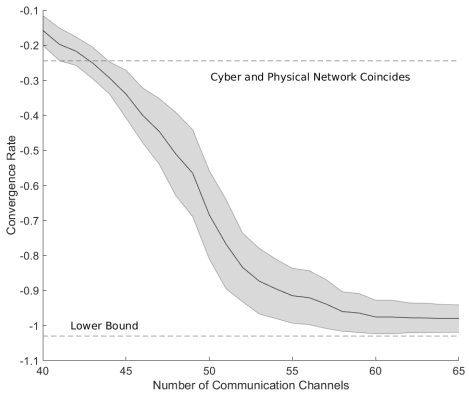

Figure 4. The convergence rate of (2) captured by the dominant real part of A as a function of the number of communication channels.

benefit on improving the system convergence from designing cyber topologies starts to flatten out and is close to the lower bound with high probability. Similar results can be observed on other IEEE testbeds and in all cases we need less than twice the number of buses to achieve near-optimal convergence with high probability. We believe this will be a good benchmark for practical applications.

VI. Conclusion

In this work, we studied the impact of cyber topology of a distributed secondary frequency control scheme on the stability, optimality and transient performance of our power system as a cyber-physical network. It was demonstrated that by carefully designing the cyber topology, near optimal convergence rate can be achieved without incurring excessive communication overhead.

This work can be extended in several directions. First, we briefly discussed two tradeoffs in Section IV in cyber network design. It is of interest to see whether such tradeoffs can be quantified so we can strike a good balance in system design. Second, many of our results rely heavily on the commutativity assumption (the homogeneity assumption in contrast is less critical) and it will be useful if this assumption can be relaxed. Finally, we are still investigating how our results can be generalized to more detailed models (say where the generators have higher order and/or nonlinear dynamics).

References

[1] A. Wood and B. Wollenberg, *Power Generation, Operation, and Control*. Wiley-Interscience, 1996.

[2] P. Kundur, N. J. Balu, and M. G. Lauby, *Power system stability and control*. McGraw-hill New York, 1994, vol. 7.

[3] B. J. Kirby, "Spinning reserve from responsive loads," *Report of Oak Ridge National Laboratory*, 2003.

[4] PNNL, "Grid friendly controller helps balance energy supply and demand." [Online]. Available: http://readthis.pnl.gov/MarketSource/ReadThis/B3099_not_print_quality.pdf

[5] J. A. Short, D. G. Infield, and L. L. Freris, "Stabilization of grid frequency through dynamic demand control," *IEEE Transactions on power systems*, vol. 22, no. 3, pp. 1284–1293, 2007.

[6] D. S. Callaway and I. A. Hiskens, "Achieving controllability of electric loads," *Proceedings of the IEEE*, vol. 99, no. 1, pp. 184–199, 2011.

[7] A. Molina-Garcia, F. Bouffard, and D. S. Kirschen, "Decentralized demand-side contribution to primary frequency control," *IEEE Transactions on Power Systems*, vol. 26, no. 1, pp. 411–419, 2011.

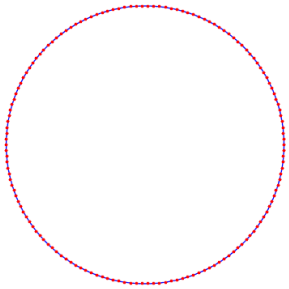

(a)

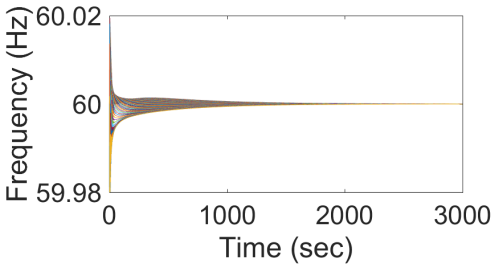

(b)

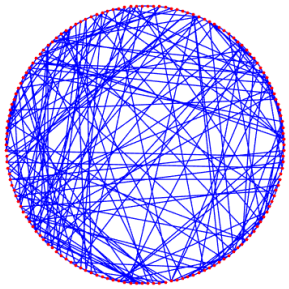

(c)

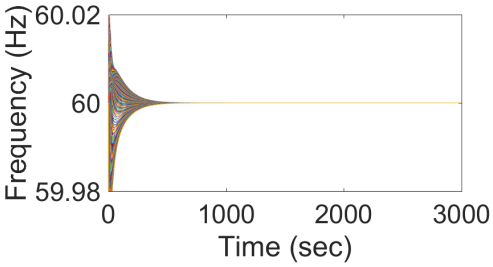

(d)

Figure 5. (a) A 300 bus ring network. (b) The frequency trajectories after a 1 pu disturbence at one bus on the ring network. (c) A small-world network with the same number of communication channels. (d) The frequency trajectories after disturbence on the small-world network.

[8] C. Zhao, U. Topcu, and S. Low, "Swing dynamics as primal-dual algorithm for optimal load control," in *Smart Grid Communications (SmartGridComm), 2012 IEEE Third International Conference on*. IEEE, 2012, pp. 570–575.

[9] C. Zhao, U. Topcu, N. Li, and S. Low, "Design and stability of load-side primary frequency control in power systems," *Automatic Control, IEEE Transactions on*, vol. 59, no. 5, pp. 1177–1189, 2014.

[10] E. Mallada and S. H. Low, "Distributed frequency-preserving optimal load control," *IFAC Proceedings Volumes*, vol. 47, no. 3, pp. 5411–5418, 2014.

[11] C. Zhao, E. Mallada, S. Low, and J. Bialek, "A unified framework for frequency control and congestion management," in *Power Systems Computation Conference (PSCC), 2016*. IEEE, 2016, pp. 1–7.

[12] A. Kasis, E. Devane, and I. Lestas, "Stability and optimality of distributed schemes for secondary frequency regulation in power networks," in *2016 IEEE 55th Conference on Decision and Control (CDC)*, Dec 2016, pp. 3294–3299.

[13] M. Andreasson, D. V. Dimarogonas, H. Sandberg, and K. H. Johansson, "Distributed pi-control with applications to power systems frequency control," in *American Control Conference (ACC), 2014*. IEEE, 2014, pp. 3183–3188.

[14] F. Dörfler and S. Grammatico, "Gather-and-broadcast frequency control in power systems," *Automatica*, vol. 79, pp. 296–305, 2017.

[15] H. Bouattour, J. W. Simpson-Porco, F. Dorfler, and F. Bullo, "Further results on distributed secondary control in microgrids," in *Decision and Control (CDC), 2013 IEEE 52nd Annual Conference on*. IEEE, 2013, pp. 1514–1519.

[16] D. K. Molzahn, F. Drfler, H. Sandberg, S. H. Low, S. Chakrabarti, R. Baldick, and J. Lavaei, "A survey of distributed optimization and control algorithms for electric power systems," *IEEE Transactions on Smart Grid*, vol. PP, no. 99, pp. 1–1, 2017.

[17] E. Mallada, C. Zhao, and S. Low, "Optimal load-side control for frequency regulation in smart grids," in *2014 52nd Annual Allerton Conference on Communication, Control, and Computing (Allerton)*, Sept 2014, pp. 731–738.

[18] L. Guo and S. Low, "Spectral characterization of controllability and observability for frequency regulation dynamics," in *Decision and Control (CDC), 2017 IEEE 56th Conference on*. IEEE, 2017.

[19] L. Guo, C. Zhao, and S. H. Low, "Graph laplacian spectrum and primary frequency regulation," *arXiv:1803.03905*.

[20] F. R. K. Chung, *Spectral Graph Theory*. American Mathematical Society, 1997.

[21] F. Paganini and E. Mallada, "Global performance metrics for synchronization of heterogeneously rated power systems: The role of machine models and inertia," in *2017 55th Annual Allerton Conference on Communication, Control, and Computing (Allerton)*, Oct 2017, pp. 324–331.

[22] M. M. Bronstein, K. Glashoff, and T. A. Loring, "Making laplacians commute," *arXiv:1307.6549*, 2013.

[23] H. Lin, "Almost commuting self-adjoint matrices and applications," *Operator algebras and their applications (Waterloo, ON, 1994/1995)*, vol. 13.

[24] S. Boyd, "Convex optimization of graph laplacian eigenvalues," in *Proceedings of the International Congress of Mathematicians*, vol. 3, no. 1-3, 2006, pp. 1311–1319.

[25] L. Guo, C. Liang, and S. Low, "Monotonicity properties and spectral characterization of power redistribution in cascading failures," in *55th Annual Allerton Conference on Communication, Control, and Computing (Allerton)*. IEEE, 2017.

[26] R. Olfati-Saber, "Ultrafast consensus in small-world networks," in *Proceedings of the 2005, American Control Conference, 2005.*, June 2005, pp. 2371–2378 vol. 4.

[27] D. J. Watts and S. H. Strogatz, "Collective dynamics of small-world networks," *nature*, vol. 393, no. 6684, pp. 440–442, 1998.

[28] R. D. Zimmerman, C. E. Murillo-Sánchez, and R. J. Thomas, "Matpower: Steady-state operations, planning, and analysis tools for power systems research and education," *IEEE Transactions on power systems*, vol. 26, no. 1, pp. 12–19, 2011.